ISSN 1819-7140, Russian Journal of Pacific Geology, 2013, Vol. 7, No. 4, pp. 247–261. © Pleiades Publishing, Ltd., 2013.
Original Russian Text © A.V. Koloskov, S.A. Khubunaya, 2013, published in Tikhookeanskaya Geologiya, 2013, Vol. 32, No. 4, pp. 24–51.

New Petrological Data on the Volcanic Rocks of the Chichinautzin Region: The Sources of the Magmatic Melts and the Origin of the Trans-Mexican Volcanic Belt

A. V. Koloskov and S. A. Khubunaya

Institute of Volcanology and Seismology, Far East Branch, Russian Academy of Sciences, bul. Piipa 9, Petropavlovsk–Kamchatskii, 683006 Russia

E-mail: kolosav@kscnet.ru

Received December 16, 2012

Abstract—New petrographic, isotopic–geochemical, and mineralogical data are presented for the volcanic rocks of the Chichinautzin region of the Trans-Mexican volcanic belt (TMVB). The geological setting and the peculiarities of the composition of the volcanic rocks from different regions of the belt are compared to the plume-related volcanic rocks from the areas of the Gulf of California, Central America, and the Galapagos hot spot. It was concluded that the composition of the intraplate rocks from the western and eastern parts of the TMVB was subjected to the Californian and Galapagos plumes, respectively. In its turn, the ascending mantle plumes provoke melting of the subcontinental lithospheric mantle related to the formation of island-arc rocks. The model of the consecutive propagating rifting in the eastward direction suggested by some researchers (Marquez et al., 1999; Verma, 2001) instead of the subduction hypothesis is in agreement with the geological and geophysical data and the isotopic–geochemical peculiarities of the volcanic rocks within the TMVB.

Keywords: petrochemistry, geochemistry, isotopy, plume reservoir, Trans-Mexican volcanic belt

DOI: 10.1134/S1819714013040052

INTRODUCTION

The Miocene–Quaternary Trans-Mexican volcanic belt is a large (up to 1000 km long and up to 200 km wide) superimposed tectono-magmatic latitudinal structure in the southern part of Northern America [35]. It is located between the Eocene–Early Miocene Sierra Madre–Occidental and Paleogene Sierra Madre–Sur provinces in the north and south, respectively (Fig. 1). The belt is divided on the blocks by numerous longitudinal and latitudinal faults with the formation of local grabens (e.g., the famous Colima graben). The occurrence of the deep trench and a zone of increased seismicity along the SW boundary of the continent suggests the possibility of the subduction of the Rivera and Cocos plates under the North American plate. The deep-seated ring structure [3] in the NW margin or slab-window structures [28] in the SE part of the reviewed region point to other factors that affect the composition and style of the local volcanism (Fig. 1). The volcanic belt includes the large unit stratovolcanoes, many large shield volcanoes, separate lava fields, and numerous lava and cinder–lava cones. The calc–alkaline series with island arc isotopic–geochemical characteristics and subalkaline–alkaline intraplate (OIB) series were distinguished among the volcanic products [18, 35, 36, 41, 56]. The first dominant type occurs everywhere in the volcanic belt and includes basalts, dacites, and rhyolites with the most abundant basaltic andesites and andesites. The felsic rocks are mostly restricted to few in number calderas [49]. The second type accompanies in various proportions the first one in all the volcanic fields, including mostly basalts with increased HFSE contents (Na, Ta, and Ti). The rocks with increased alkalinity are widespread in the western (basanites, leucitites, and lamprophyres) and eastern (trachybasalts and hawaiites) parts of the belt [12, 13, 21, 31, 34].

Although the reviewed volcanic belt is well studied and described in numerous publications, there is no consensus on its origin. The reason for this is probably a series of peculiarities that differ it from typical volcanic belts of active continental margins (e.g., see [45] for the southern part of South America): (1) the belt is oriented at an angle of 15–20° to the strike of the Middle American deep trench; (2) the location of the subduction slab deeper than 50 km is unclear [53]; (3) due to the absence of transverse zoning of the volcanic fields typical of many convergent systems, the alkaline series are manifested in the marginal parts of the belt [21, 23, 34]; (4) the caldera and stratovolcanoes are dispersed along the entire volcanic belt, although usually they strongly dominate in the frontal part of the active continental margin [45]; and (5) the series of isotopic–geochemical features do not allow us to

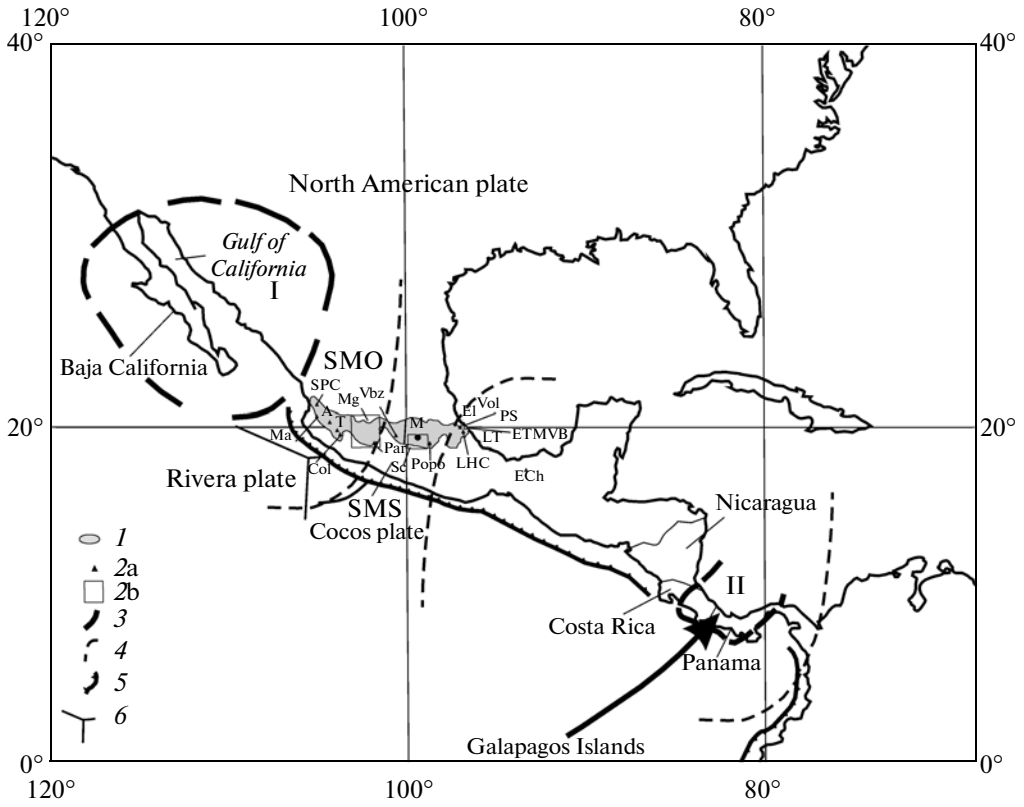

Fig. 1. Location of the Trans-Mexican Volcanic Belt (TMVB). (*1*) the TMVB; (*2*a, *2*b) the local and areal volcanic fields: (SPC) San Pedro–Ceboruco, (Ma) Mascota–San Sebastian, (A) Ayutla, (T) Tapalpa, (Col) Colima–Cantaro, (Mg) Michoacán–Guanajuato, (Par) Paricutin, (Vbz) Valle de Bravo–Zitácuaro, (Sc) Sierra Chichinautzin, (M) Mexico, (Popo) Popokatepetl, (El Vol) El Volcancillo, (ETMVB) eastern flank of the TMVB, (PS) Palma Sola, (LHC) Los Humeros, (LT) Los Tuxtlas, and (ECh) El Chichón; (*3*) the Californian ring structure (I) and the Galapagos slab window (II); (*4*) the inferred boundaries of the influence of the mantle plumes (based on the isotopic data); (*5*) deep trenches; (*6*) boundaries of the tectonic plates. The volcanic provinces: (SMO) Sierra Madre–Occidental, (SMS) Sierra Madre–Sur. The arrow indicates the direction of the movement of the plume's source.

relate the volcanism with the subduction of the Cocos or Rivera plates [35, 37, 48].

All of these produced different points of view on the origin of the belt: (1) traditional subduction [9, 22, 31] complicated by intrusion of the astenospheric component into the mantle wedge [13, 18, 56] and the relation to (2) mantle plumes [35, 38] or (3) rifting [35, 36, 48, 51, 56].

Such ambiguity allows the consideration one more time of the conditions of the volcanism within the TMVB based on new data and the analysis of the published literature.

FACTUAL MATERIAL AND METHODICAL PREREQUISITES

In 1984, one of the authors of the present paper had occasion to take part in field geological and tephrochronological studies in the territory of Mexico. The works were organized by the Institute of Geophysics of the UNAM within the framework of the scientific collaboration with Mexican scientists. The studies covered the central part of the Chichinautzin field and also a series of fields in the neighborhood of Mexico City. In the course of these works, a geological map (Fig. 2) and a working stratigraphic scheme were composed and a vast amount of samples were collected, the results of the investigations of which are presented in the given paper.

The contents of the rare and rare earth elements were analyzed at the Max Plank Institute for Chemistry (Mainz, Germany) and supported by the A.V. Sobolev grant within the project of Paul Wolfgang. The rocks were powdered and sintered into a glass using an Ir heater [46]. The contents of the elements in the glasses were determined using laser ablation inductively coupled plasma mass spectrometry (LA ICPMS) using an ELEMENT-2 mass spectrometer (Thermo Scientific, UK) equipped with a UP-213 New Wave Research solid-state laser (UK). The KL-2G and NIST 612 basaltic glass were used as standards [27]. The typical diameter of the crater in the glass after the laser ablation was 60–80 μm, and the time of the ablation was 60–80 s. The error of the anal-

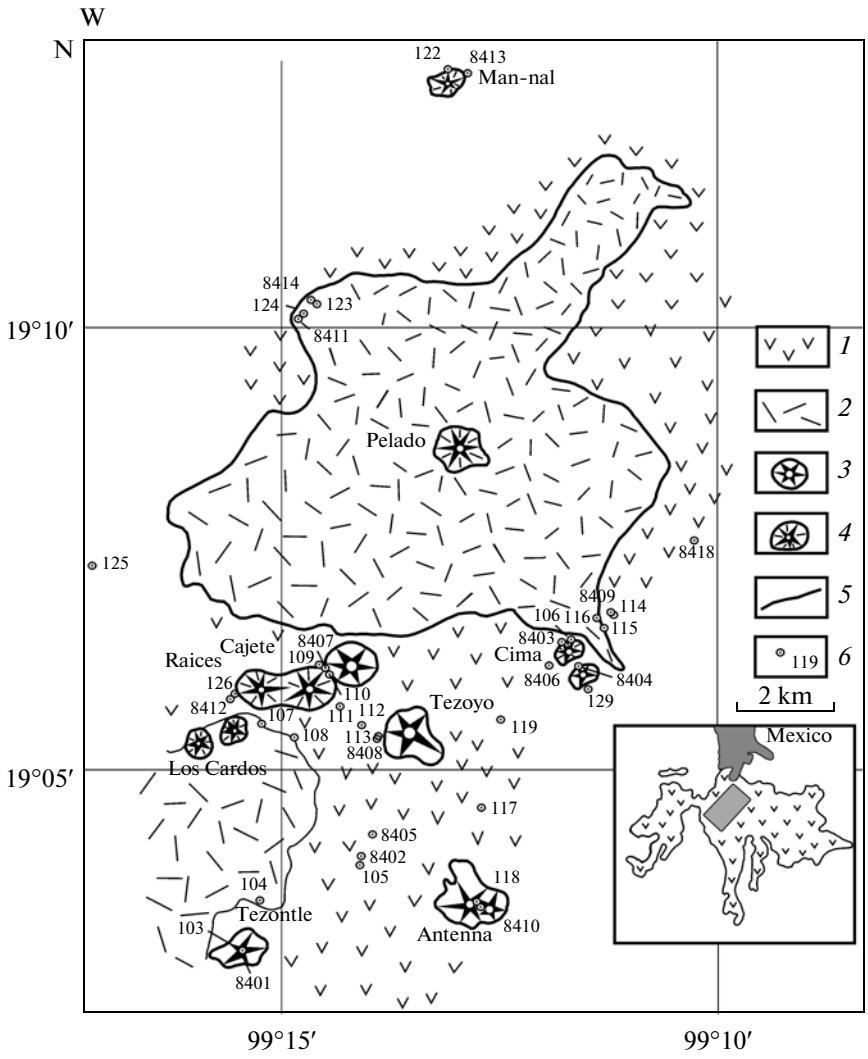

Fig. 2. Geological scheme of the Chichinautzin area modified after [1]. (*1–2*) volcanic flows; (*3–4*) cones of the first (*1*, *3*) and second (*2*, *4*) volcanic cycles, (*5*) geological boundaries, (*6*) observation points. The inset map shows the location of the studied area within the Sierra Chichinautzin volcanic field.

ysis estimated by the standard reproduction was <5 rel % (two standard errors) for contents of >1 ppm and 10 rel % for contents of ~0.1 ppm.

The Sr and Nd isotopic composition was determined at the Institute of Geochemistry and Analytical Chemistry of the Russian Academy of Sciences (GEOKHI RAS, Moscow, analyst S.F. Karpenko) on a modified TSN 206 SA mass spectrometer with a three-banded ion source. The measured Nd isotope ratios were normalized by $^{150}Nd/^{142}Nd = 0.209627$ using $(^{143}Nd/^{144}Nd)_{chur} = 0.512638$. The Pb isotopic content was measured on a Finnigan Mat-262 mass spectrometer in the Baikal Center for Collective Use of the Siberian Branch of the Russian Academy of Sciences in Irkutsk. The accuracy of the analysis was controlled by measurements of the NMS-981 international standard ($^{206}Pb/^{204}Pb = 16.937$; $^{207}Pb/^{204}Pb = 15.491$; $^{208}Pb/^{204}Pb = 36.6280$). The same analyses for the same samples were duplicated at the GEOKHI RAS (analyst S.F. Karpenko). The precision of the analyses was 0.006 for $^{206}Pb/^{204}Pb$, 0.010 for $^{207}Pb/^{204}Pb$, and 0.050 for $^{208}Pb/^{204}Pb$.

The composition of the minerals was analyzed using a CAMEBAX microprobe at the Institute of Volcanology and Seismology of the Far East Branch of the Russian Academy of Sciences. The precision of the analysis was ~0.1% for the oxides and ~10% for the trace elements.

PECULIARITIES OF THE VOLCANISM OF THE CHICHINAUTZIN FIELD

The Chichinautzin field occupies the central part of the Trans-Mexican volcanic belt (TMVB) (Fig. 1). The belt began to form in the Early Miocene, and its maximum volcanic activity occurred ca. 20–15, 9–6

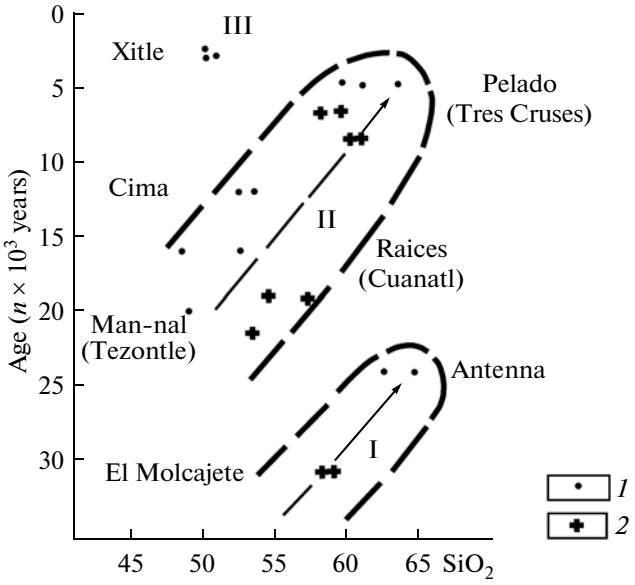

Fig. 3. SiO_2 content–age dependence of the rocks from the Chichinautzin region. The data from [1] (*1*) and [10] (*2*). (I, II, III) volcanic cycles.

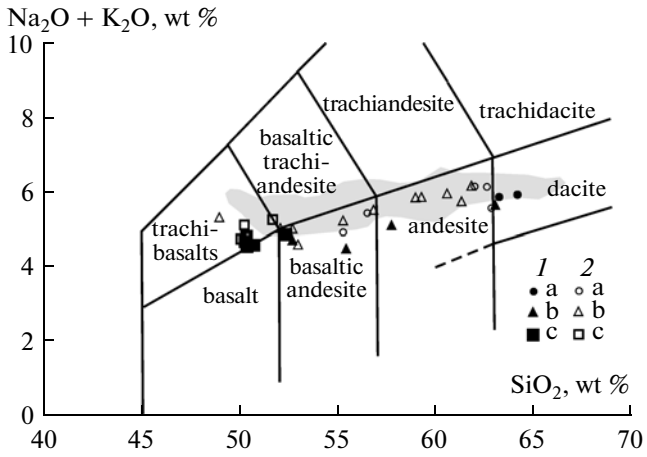

Fig. 4. $Na_2O + K_2O/SiO_2$ plot for the rocks of the Chichinautzin region based on the data from Table (*1*) and the previous studies of the authors (*2*) according to the different volcanic cycles: (a) I, (b) II, (c) III. The composition field is designated after [56].

Ma, and 3–0 Ma ago. During the evolution, the volcanism gradually moved from the north to the south [9]. The volcanic activity in the reviewed zone spans the period from the Late Pliocene–Pleistocene till the present [39]. The age data [1], along with the composition of the rocks, allowed us to distinguish three clearly expressed basic-to-acid volcanic stages within the studied region (Fig. 3). The lavas and pyroclastic rocks of the large Pelado shield volcano and seven volcanic cones were studied in the reviewed zone (Fig. 2). The studies covered several cones in the area of Mexico City too.

PETROGRAPHY AND MINERALOGY OF THE ROCKS

Olivine basalts and andesites; pyroxene andesites and dacites; and mixed lavas (andesites and dacites) with plagioclase, biotite, and hornblende phenocrysts are distinguished in the Sierra–Chichinautzin volcanic field [35]. The coexistent olivine and quartz xenocrysts are typical of many samples, some of which contain aggregates of plagioclase or quartz and quartz–plagioclase (granite) xenoliths [56].

Generally, the aphyric volcanic rocks of the reviewed region contain rare olivine, plagioclase, and pyroxene phenocrysts or subphenocrysts.

The composition of the rocks of the first volcanic cycle varies from basaltic andesites to dacites (Figs. 3, 4). More felsic rocks are confined to the cones, whereas more mafic rocks with an increased amount of phenocrysts (locally, up to 10–15%) are exposed in the basement of the cones or observed in the related flows. The andesites of a nameless cone northeast from the Cajete cone contain up to 5–7% plagioclase megacrystals, single amphibole phenocrysts (sample 109), and quartz inclusions up to several millimeters in size. The rocks of this cycle with a dominant hyalopilitic texture are typically poorly devitrificated.

The composition of the rocks of the second more complete cycle varies from basalts to dacites (Figs. 3, 4). The porous poorly devitrificated basalts of the Man-nal cone host up to 5–7% olivine and clinopyroxene phenocrysts and subphenocrysts. The matrix contains up to 60% brown glass and small poorly individualized crystallites of clinopyroxene, plagioclase, and olivine. The basaltic andesites of the Cima cone host single phenocrysts–subphenocrysts of olivine, plagioclase, clino- and orthopyroxene, or their intergrowths. The felsic aphyric andesites of the Pelado volcano are characterized by single phenocrysts–subphenocrysts of olivine, clinopyroxene, and orthopyroxene, and plagioclase and quartz–feldspar inclusions up to 5–8 cm in size. The matrix contains up to 30% brown glass overcrowded by plagioclase and clinopyroxene crystallites and also microlites of these minerals and orthopyroxene. Generally, the second volcanic stage is characterized by an increase in the degree of devitrification as far as the SiO_2 content increases and also an increase in the amount of ortopyroxene both among the phenocrysts and microlites.

The monotonous basalts of the third volcanic cycle strongly differ by their petrography and petrochemistry from the same rocks of the first and second cycles. They are characterized by high TiO_2 and slightly higher Al_2O_3 contents and considerably lower SiO_2 and K_2O contents. The nearly completely devitrificated rock matrix contains 5 to 10% phenocrysts–subphenocrysts of olivine, plagioclase, and rare clinopyroxene; these rocks are almost dolerites. Orthopyrox-

ene and amphibole are completely absent. The glass content in the rock is 3–5%. The membranous glass is locally developed near the pores or mineral boundaries. The rock is mostly composed of long plagioclase laths (60–70%) with interstitial grains of olivine, clinopyroxene, and magnetite.

Olivine is a common mineral of the phenocrysts–subphenocrysts almost of every rock. The most magnesium olivine (cores of phenocrysts) typically corresponds to $Fo_{82–86}$ in composition. However, magnesium olivine of $Fo_{89–90}$ in composition was found in basaltic andesites of the Los Cardos cone (Fig. 5). Similar anomalous compositions were identified in the basaltic andesites of the cinder cones of the eastern part of the reviewed region [37] and also the Mascota and San Sebastian volcanic fields in the west of the TMVB [31]. Such compositions may be explained by the water-saturated parental melts and the higher oxidized conditions of the crystallization [37]. Toward the marginal zones of the phenocrysts, the composition of the olivine becomes more ferroan with a simultaneous increase in the MnO and CaO contents, approaching the composition of the microlites ($Fo_{67–62}$) (Fig. 5). However, in some basaltic andesites (samples 108 and 109), this zoning is limited by orthopyroxene (rims around the olivine grains) and the olivine is $Fo_{74–70}$ in composition. The basalts of the third cycle devoid of orthopyroxene have more ferroan olivine up to Fo_{46} in composition (Fig. 5). Numerous inclusions of Cr–Al spinels in the olivine are typical of the basaltic andesites of the first and second cycles. The olivine from the basalts of the third cycle is almost free of these inclusions.

The orthopyroxene in the basaltic andesites occurs as zonal subphenocrysts with the maximum magnesium composition of $En_{86–81}$, small grains in the rock matrix ($En_{76–72}$), and rims around olivine grains with the maximum ferroan composition of $En_{66–71}$. It is interesting that the most magnesium orthopyroxene was found in the samples with the most magnesium olivine (sample 104).

The clinopyroxene from phenocrysts, subphenocrysts, and cores of microlites generally is similar in composition. The zoning is expressed in an increase in the iron mole fraction in the marginal zones (from 15–16 to 26–28 in the basaltic andesites and from 20 to 44 in the basalts). Commonly, the TiO_2 and Na_2O contents also slightly increase. The CaO content significantly decreases in the marginal zones of some microlites (sample 109), especially in the intergrowths with orthopyroxene, which also resulted in the appearance of pigeonite at the contact. The composition of the clinopyroxene of the third cycle is distinct in its higher iron mole fraction and Al_2O_3 and Na_2O content and high TiO_2 content.

The feldspar is plagioclase, and one sample of the basalt of the third cycle (sample 120) contains anorthoclase rims. It is worth noticing that the most calcic

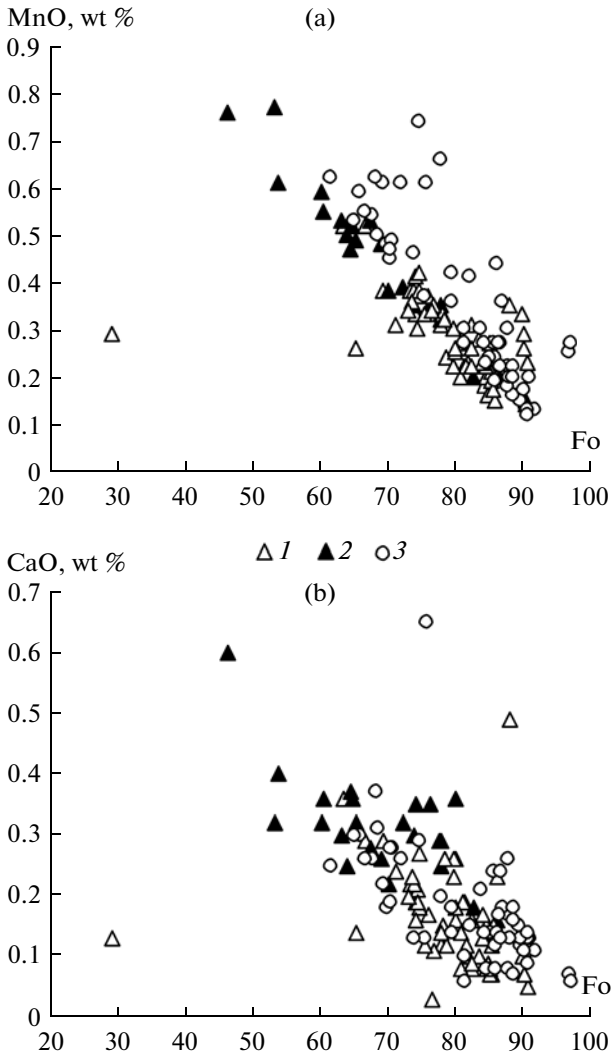

Fig. 5. Fo–MnO (a) and Fo–CaO (b) correlation in olivine from the Chichinautzin area. (*1*) Island arc basalt (cycle II), (*2*) intraplate basalt, cycle III, (*3*) island arc volcanic rocks of Mascota–San Sebastian [31]. Fo = Mg/(Mg + Fe).

compositions ($An_{71–63}$) were identified not only in the basalts of the third cycle but in the more felsic basaltic andesites of the first and second volcanic cycles. The composition of the plagioclase in the cores of the phenocrysts from the basalts of the third cycle corresponds to $An_{59–55}$. The composition of the mineral varies in the marginal zone from $An_{56–54}$ to $An_{49–43}$ in the basaltic andesites and is $An_{52–44}$ in the basalts.

Based on the analysis of single phenocrysts, the amphibole corresponds to Fe–Ca kaersutite with a higher TiO_2 content. The marginal zones are characterized by an increased iron mole fraction and decreased Na_2O and TiO_2 contents.

The mineralogy of the volcanic rocks of the different cycles indicates the most significant differences between the basalts of the third cycle and the abundant

basaltic andesites of the first and second cycles. The compositions of the olivine and pyroxene from the younger volcanic rocks widely vary in contrast to the limited compositions of the feldspar. An opposite picture, as a rule, is observed for the early two cycles. This is well in agreement with the consequences of the mineral crystallization: the major mass of plagioclase in the basalts of the late cycle is formed before the dark-colored minerals in contrast to the basaltic andesites.

PECULIARITIES OF THE RARE ELEMENT AND THE ISOTOPIC COMPOSITION OF THE ROCKS

New data on the petrochemical, rare element, and isotopic composition are shown in the table for representative samples of different volcanic cycles of the Chichinautzin zone. In spite of the more complete set of components in the table and the different analytical methods used for the major oxides, they are well comparable to the data of previous researchers [54, 55] for the same cones and volcanoes. Based on [56], the SiO_2 content in the large sampling of the rocks from the Chichinautzin field varies from 49.9 to 65.2 wt %. The total alkalinity ranges from 5–7 to 6–7 wt %. The compact field of the data points with direct correlation is observed on the corresponding plot (Fig. 4). Alkaline and subalkaline types were distinguished among these rocks by previous researchers. Although the alkaline rocks and calc-alkaline rocks with the lowest SiO_2 content are similar by the contents of the major oxides, they are significantly distinct in their TiO_2, Nb, and Zr contents at several intermediate values [56]. The composition of the rocks of the first and second cycles corresponds to the calc–alkaline type and that of rocks of the third cycle, to the alkaline type (table). The first and second types are island arc (supra-subduction) and intraplate geochemical types, respectively. As seen from the table, these types differ by the Ta, Y, Yb, and Lu contents and also by the La, Ce, Zr, and Hf contents at similar alkalinity and SiO_2 content. The island arc type is considerably enriched in radiogenic Sr at a similar Nd and Pb isotopic composition.

DISCUSSION

The genetic problems of the volcanic rocks of the Chichinautzin region need to be considered within the entire Trans-Mexican volcanic belt. Thus, we will briefly consider the rock composition in the individual regions.

MAIN REGULARITIES OF THE TMVB VOLCANISM

Petrographic Types of the Rocks

Let us consider how the composition of the volcanic rocks varies along the strike of the belt (Fig. 1). The Mascota–San Sebastian region is a western part of the TMVB distinct in composition and the type of volcanism from the NW block. The latter is a series of mostly large andesite stratovolcanoes located along the Tepic–Zacoalco rift zone. The coexisting calc-alkaline and intraplate Na-alkaline (OIB) volcanism was identified in the San Pedro–Ceboruco graben in the NW block [41].

The Mascota–San Sebastian region is characterized by small Late Pliocene–Quaternary volcanic centers of high K-alkali basanites and lamprophyres (minettes, absarokites, leucitites, spessartites, and kersantites) combined with calc-alkali basaltic andesites [12, 31, 34].

The Pliocene–Quaternary Ayutla and Tapalpa lava fields [42] located somewhat eastward include alkaline intraplate (alkali basalts and hawaiites), potassium (trachilavas and lamprophyres), and calc-alkaline series.

The Quaternary volcanism of the Colima–Cantaro region is interested, first, by the rapid (1.7 Ma) shift of the volcanic front to the south and, second, by its tectonic location at the boundary of the Rivera–Cocos oceanic plates and as a part of the triple rift system in the west of the TMVB [54]. The large volcanic centers (the Colima, Nevado de Colima, and Cantaro) are characterized by calc-alkaline and subalkaline series (from trachibasalts to dacites), whereas numerous small surrounding cones vary from basanites to lamprophyres.

The large Michoacan–Guanajuato volcanic province is located further to the east and includes numerous lava and cinder cones (two of which in the southern part (the Paricutin and Jorullo) were formed in the historical time), lava cupolas, maars, small shield volcanoes, and separate lava fields [25, 31, 43]. They include calc-alkali basalts, basaltic andesites, and andesites with subordinate alkaline rocks. The lava of the Paricutin volcano corresponds to the basic-to-acid calc-alkaline series from basaltic andesites to andesites. The numerous crustal xenoliths and the direct $^{87}Sr/^{86}Sr–SiO_2$ correlation were the reason to consider this volcano as a classical example of crustal contamination [43].

The similar vast Valle de Bravo–Zitácuaro province with numerous lava–cinder cones and separate volcanic fields formed 6 Ma to 5 ka ago is situated further to the east [22]. The volcanic rocks are referred to the typical island arc calc-alkaline (basaltic andesite–dacitic andesite) series, although some compositions with a higher K_2O content were identified as shoshonites.

The central block of the reviewed consequence is characterized by dominant calc-alkaline rocks—products of the areal and focused volcanism [10, 48, 56, and our data]. The active and famous Popokatepetl stratovolcano with calc-alkaline series from basalts to dacites located southeast from this province should also be noted [44].

Petrochemical, geochemical, and isotopic composition of the rocks of the Chichinautzin region and Mexico City

Number of sample	MX 102	MX 120	MX 121	MX 127	MX 106	MX 122	MX 108	MX 124	MX 105	MX 118
No.	1	2	3	4	5	6	7	8	9	10
SiO_2	50.32	50.45	50.73	52.42	52.70	55.44	57.70	62.97	63.24	64.16
TiO_2	1.75	1.72	1.72	1.71	1.37	0.88	0.93	0.92	0.78	0.74
Al_2O_3	16.00	15.99	16.32	15.74	16.66	15.38	16.21	15.96	15.51	15.45
FeO	8.65	8.73	8.06	8.37	8.24	6.68	6.20	5.01	4.63	4.96
MnO	0.16	0.16	0.16	0.15	0.16	0.12	0.12	0.12	0.09	0.10
MgO	8.02	8.88	8.18	7.57	7.30	8.73	6.45	3.73	3.97	3.74
CaO	8.28	8.22	8.27	7.34	7.53	6.79	6.67	5.01	4.97	4.66
Na_2O	3.59	3.51	3.54	3.58	3.71	3.30	3.76	3.90	3.67	3.76
K_2O	1.08	1.02	1.04	1.26	0.97	1.16	1.32	1.72	2.21	2.16
P_2O_5	0.48	0.39	0.43	0.50	0.24	0.17	0.24	0.21	0.23	0.22
Total	98.32	99.08	98.46	98.65	98.88	98.65	99.60	99.54	99.29	99.95
Rb	17	17	16	21	19	27	28	42	54	58
Ba	277	271	259	366	231	312	417	536	619	629
Th	2.17	2.14	2.24	3.14	1.89	1.99	3.23	4.50	5.54	5.65
U	0.62	0.61	0.53	0.70	0.57	0.64	0.91	1.12	1.55	1.52
Nb	19.6	19.7	18.4	25.2	11.5	4.9	6.2	11.2	8.7	8.7
Ta	1.19	1.18	1.16	1.55	0.75	0.34	0.40	0.72	0.60	0.62
La	21.53	20.58	20.55	28.88	13.61	11.75	18.40	23.06	26.21	25.36
C	45.44	44.27	42.11	55.80	28.73	24.19	38.68	44.48	51.98	50.74
Pb	5.8	2.4	5.0	1.9	2.7	2.9	4.7	5.7	5.4	5.1
Pr	5.99	5.69	5.76	7.58	3.88	3.36	5.17	5.61	6.46	6.07
Nd	26.66	25.72	26.92	34.55	18.40	15.52	22.99	24.20	27.24	25.54
Sr	518	525	523	496	431	382	540	434	384	350
Sm	5.91	5.65	6.03	7.48	4.42	3.66	4.99	4.92	5.32	4.94
Zr	228	222	221	327	168	148	164	226	230	230
Hf	3.90	4.18	4.29	6.36	3.37	3.17	3.38	4.82	4.73	4.61
Eu	1.82	1.81	1.92	2.18	1.40	1.17	1.39	1.36	1.34	1.18
Cd	5.38	5.18	5.69	7.35	4.42	3.47	4.16	4.44	4.37	4.15
Tb	0.79	0.80	0.85	1.06	0.69	0.52	0.59	0.62	0.60	0.58
Dy	5.03	5.01	5.51	6.93	4.43	3.41	3.64	3.94	3.65	3.52
Ho	0.97	0.99	1.06	1.34	0.85	0.67	0.69	0.74	0.69	0.67
Y	26	25	26	33	23	17	19	19	18	18
Er	2.70	2.74	3.00	3.84	2.42	1.90	1.92	2.13	1.93	1.91
Tm	0.38	0.40	0.43	0.51	0.34	0.27	0.27	0.29	0.26	0.26
Yb	2.60	2.62	2.83	3.47	2.29	1.73	1.86	2.02	1.79	1.75
Lu	0.37	0.38	0.41	0.52	0.33	0.25	0.27	0.29	0.26	0.26
Ni	159	193	172	166	138	230	133	61	86	74
Sc	25	25	27	25	23	23	20	15	15	16
Co	36	39	36	30	33	32	24	16	16	16
Li	8.23	8.63	8.65	9.88	9.24	11.10	13.00	18.80	19.23	21.60
V	144	164	165	140	134	111	111	86	82	83
$^{87}Sr/^{86}Sr$	0.703599	no	no	no	no	0.704008	0.704368	no	no	no
$^{143}Nd/^{144}Nd$	0.512895	no	no	no	no	0.512921	0.512868	no	no	no
$^{206}Pd/^{204}Pd$	18.687	no	no	no	no	18.573	18.635	no	no	no
$^{207}Pb/^{204}Pb$	15.576	no	no	no	no	15.556	15.563	no	no	no
$^{208}Pb/^{204}Pb$	38.381	no	no	no	no	38.236	38.330	no	no	no

Note: The sampling location: (1–4) the area of Mexico City; (5–10) the area of the Chichinautzin region (see Fig. 2), the cones: (5) the Cima, (6) the Man-nal, (7) the Los Cardos, (8) the Pelado volcano, and (9–10) the Antenna cone. The volcanic cycles: (9–10) I, (5–8) II, (1–4) III.

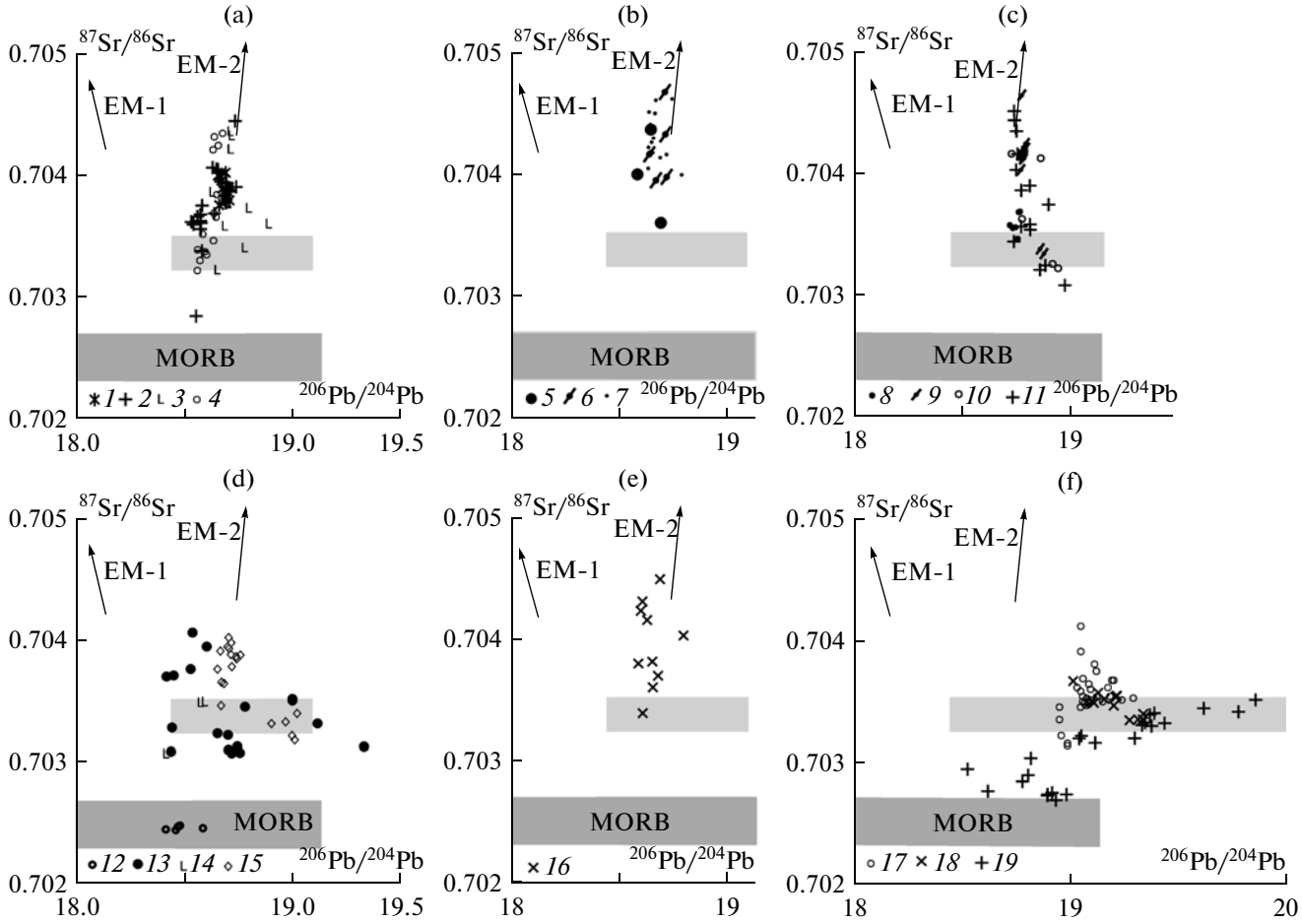

Fig. 6. $^{87}Sr/^{86}Sr$ and $^{206}Pb/^{204}Pb$ isotope ratios for the volcanic rocks from different regions of the TMVB and the adjacent territory. (a) Western part of the TMVB: (*1*) Mascota–San Sebastian [23, 32]; (*2*) Colima–Cantaro [32, 54]; (*3*) Michoacán–Guanajuato [53]; (*4*) Valle de Bravo [22]; (b) central part: (*5–6*) Chichinautzin: (*5*) Table, (*6*) [48]; (*7*) Popokatepetl [44]; (c) part: (*8*) El Volcancillo [13]; (*9*) Los Humeros [49]; (*10*) Los Tuxtlas [51]; (*11*) Palma Sola [21]; (d) California: (*12*) California Gulf, submarine Alarcon Ridge [14]; (*13–14*) Baja California: (*13*) tholeiitic, calc-alkaline, and Nb-basalt [6, 7, 32]; (*14*) bajaite (adakite) [6]; (*15*) San Pedro–Ceboruco [41]; (e) central part, longitudinal intersection: (*16*) geotraverse 100° W [9]; (f) Central America, Galapagos Islands: (*17*) Nicaragua, Costa Rica, Panama—alkaline basalt [19]; (*18*) Costa Rica, Panama–adakite [19]; (*19*) Galapagos Islands [20, 30]. The GEOROC data base is used. The lower field—the Pacific Ocean MORB [2, 54]; the upper field—the inferred composition of the plume's source. EM-1 and EM-2 are enriched mantle reservoirs [26].

The eastern block of the TMVB is less studied. The Late Miocene calc-alkaline volcanism ca. 7.5 Ma ago changed to mafic alkaline OIB-like volcanism in the eastern flank of the belt [40]. A combination of calc-alkaline and alkaline rocks (alkali basalts, hawaiites, and mugearites) is recorded in separate flows and cones in the El Volcancillo area [13]. The extreme NW area of the TMVB represents Miocene–Pleistocene alkali platobasalts and Quaternary calc-alkaline cinder cones of the Palma Sola volcanic field [21]. Finally, work [51] demonstrates the results of the isotopic–geochemical analysis of several samples of alkali basalts and basanites (melanephelinites) from the Los Tuxtlas and El Chichón regions located separately southwest of Mexico (Fig. 1).

ISOTOPIC COMPOSITION OF THE VOLCANIC ROCKS

Let us estimate the role of various sources that affect the composition of the TMVB volcanic rocks on the basis of plots of the combined Rb–Sr and U–Th–Pb isotopic systems (Fig. 6). The plots are grounded based on the comparison of the data on the isotopic composition of the volcanic rocks from the western flank of the belt (Fig. 6A) and the Gulf of California (Fig. 6D) and also those of the eastern flank of the belt (Fig. 6C) and Central America and the Galapagos archipelago (Fig. 6F). The data on the remaining part of the TMVB volcanic rocks (Fig. 6B) and the geotraverse along 100° W (Fig. 6E) occupy the central part.

Some models estimate the value of the plume–astenospheric source based on the curve, flattening, or junction of the trends on similar plots if the composition of the volcanic rocks presumably of the mantle genesis changes [57, 58]. The composition of the plume source approximately in the same range of values ($^{87}Sr/^{86}Sr = 0.70325–0.70352$) may be estimated both for the Galapagos and California plumes (Figs. 6D and 6F). The idea concerning the Galapagos plume (hot spot) and its participation in the formation of the volcanic rocks of the aseismic Cocos and Carnegie ridges [24] and the Quaternary alkali basalts of Nicaragua, Costa Rica, and Panama are considered to be rather substantiated. The isotope ratios for the Galapagos plume's source were determined as 0.70328 ($^{87}Sr/^{86}Sr$) and 18.9 ($^{206}Pb/^{204}Pb$) [24], which quite corresponds to the area conditionally designated on the plots (Fig. 6). The plume's reservoir is well expressed in Fig. 6F both in the composition of the volcanic rocks from the Galapagos archipelago and Central America.

Similar Sr isotopic markers may be observed in the composition of the volcanic rocks from Baja California (Fig. 6D), which are very similar to Central America [7]: the astenospheric slab window, the aseismic ridge, and similar rocks (high-Nb basalts associated with Mg basaltic andesites–adakites–bajaites) with close isotopic characteristics. As seen from Fig. 6D, the plume source is also well manifested for the volcanic rocks of the San Pedro–Ceborucco graben (the NW end of the TMVB): the $^{87}Sr/^{86}Sr$ ratio of 0.70344 separates the Na-alkali intraplate and calc-alkali basalts with highly radiogenic Sr. Thus, we confirmed the possible relation of the Na-alkaline magmas of this region to the mantle plumes suggested before [35, 38].

As to the major part of the TMVB volcanic rocks (Figs. 6A and 6B), the dominant data points of the calc-alkali volcanic rocks from the Mascota area (including one point of lamprophyre); the Colima and Popokatepetl volcanoes; and the Michoacán–Guanajuato, Valle de Bravo–Zitácuaro, and Chichinautzin lava fields form a compact vertical band above the plume marker. They form a single trend corresponding to the change in the compositions of the enriched mantle component of the EM-2. The intraplate basanites with higher TiO_2 and high Nb and Ta contents occur among the alkaline rocks of the Michoacán–Guanajuato region. Based on the Sr and Pb ratios, they belong to the field of the compositions with typical plume markers (Fig. 6A). Some points of the isotopic compositions of the andesites from the Valle de Bravo–Zitácuaro and Cantaro–Colima regions are also located in this field, however, without the trend curve and the typical intraplate geochemical characteristics. The $^{87}Sr/^{86}Sr$ ratio of 0.703599 (table) for the Chichinautzin area only approaches that of the plume field, although it corresponds to the transition to the intraplate rocks (Fig. 6B). No traces of the plume reservoir are present here. The longitudinal intersection of the TMVB (Fig. 6E) testifies to the mostly radiogenic Sr isotopic composition of the high-K basaltic andesites and the andesites of the frontal zone in comparison to the high-Ti (intraplate) basalts and basaltic andesites of the rear zone, but this difference is unclear due to the gradual transitions.

Further to the east (Fig. 6C), we record the plume component in the composition of the intraplate basanites (melanephelinites) of the Los Tuxtlas, the alkali basalts of the El Chichón [51], the alkali platobasalts and basanites from the Palma Sola [21], and the volcanic rocks of the Los Humeros caldera complex [49]. The hyperstene-normative basalts of the latter without an Nb-minimum likely correspond to the intraplate (riftogenic) rather to the island arc (subduction) type. Probably, the plume source is also related to the composition of the hawaiites of the El Volcancillo region at the eastern front of the TMVB, because they are also intraplate and their Sr isotopic compositions are close to the boundary of the plume reservoir. The calc-alkali basalts and basaltic andesites of the Palma Sola area and the trachiandesites of the Los Humeros caldera form a subvertical trend with slightly higher $^{206}Pb/^{204}Pb$ ratios relative to the dominant data points for the rest of the TMVB rocks.

As shown in Fig. 6, no lithospheric source of the oceanic crust (MORB) participated in the composition of the TMVB rocks, although it is well manifested in the volcanic rocks both of the California and Galapagos regions.

Proportion of Index Elements

The comparative plots with the fluid- and melt-mobile elements are well informative for the interpretation of the geochemical data. One of the examples is the Nb–K plot, which will be used for the comparison of the data on various TMVB regions (Fig. 7).

As seen from Fig. 7A, the data points of the composition of the calk-alkaline rocks from the western block of the TMVB (the Mascota–San Sebastian, Ayutla, Tapalpa, Colima, and Paricutin volcanoes and the Valle de Bravo–Zitácuaro lava field) are located in the island arc field with typical direct Nb–K correlation. The alkaline rocks form common trends going beyond the limits of this field. This correlation is also disturbed for some alkali olivine basalts and hawaiites of the Ayutla, Tapalpa, and Colima volcano areas. The subvertical trend appears toward the field of the Hawaiian basalts, being especially clearly manifested in the Nb-enriched basalts of the Michoacán–Guanajuato volcanic field with plume isotopic characteristics (Fig. 6A). These peculiarities indicate the intraplate volcanism.

Some papers [3, 31] emphasize the different degree of water saturation and oxidation during the evolution of the magmatic system. Along with H_2O-bearing minerals (amphibole and biotite), these are the sup-

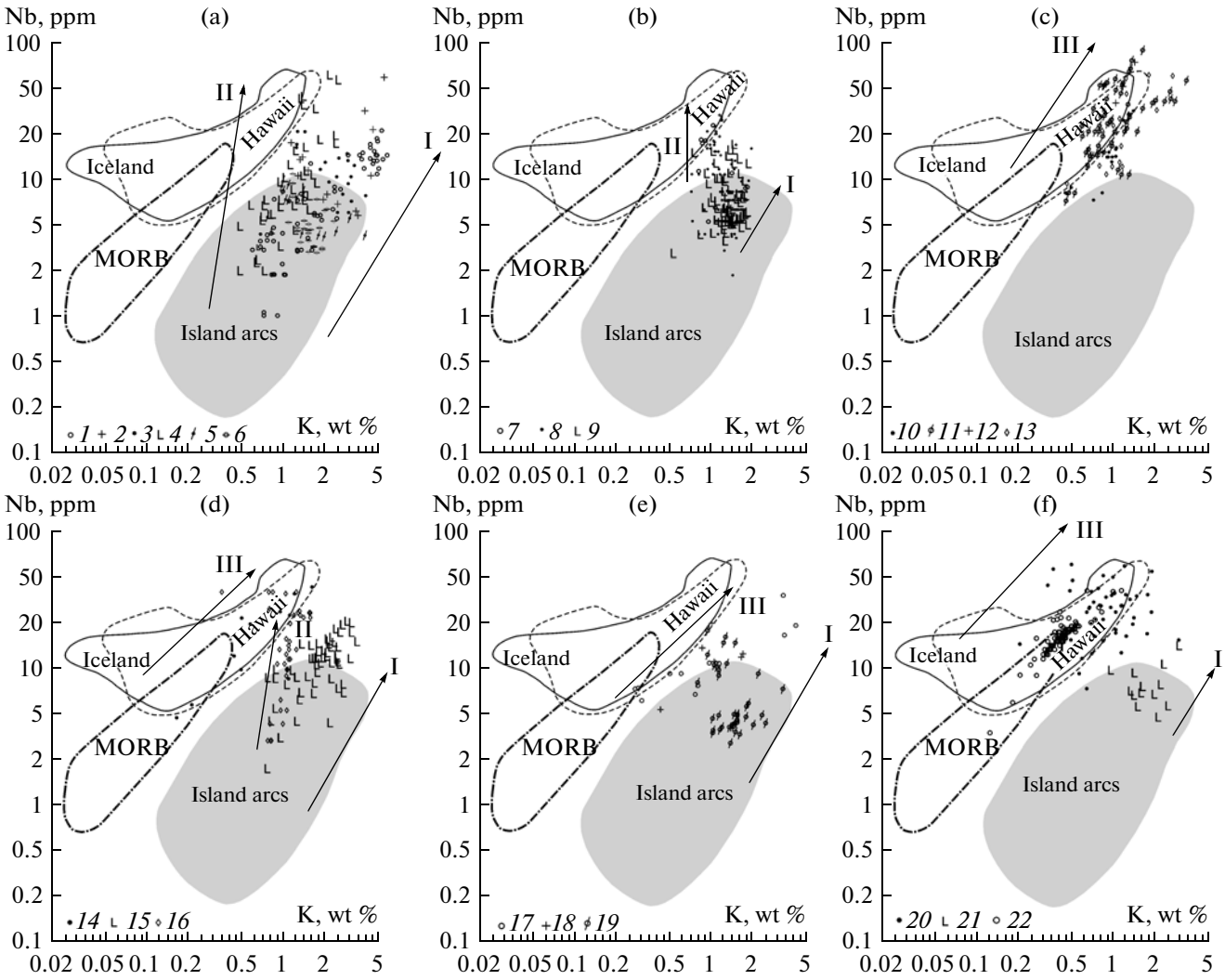

Fig. 7. Nb–K correlation for the volcanic rocks from different regions of the TMVB and the adjacent territory. (a) Western part of the TMVB: (*1*) Mascota–San Sebastian [12, 23, 31], (*2*) Ayutla, Tapalpa [42], (*3*) Colima–Cantaro [32, 35], (*4*) Michoacán–Guanajuato [15, 25, 53], (*5*) Paricutin volcano [43], (*6*) Valle de Bravo–Zitácuaro [22]; (b) central part: (*7–8*) Chichinautzin: (*7*) Table, (*8*) [48, 56], (*9*) Popokatepetl [44]; (c) eastern part: (*10*) El Volcancillo [13], (*11*) eastern flank of the TMVB [40], (*12*) Los Tuxtlas [51], (*13*) Palma Sola; (d) California: (*14–15*) Baja California: (*14*) tholeiitic, calc-alkaline, and Nb-basalt [6, 7, 32], (*15*) bajaite (adakite) [6, 7, 11], (*16*) San Pedro–Ceboruco [41]; (e) central part, longitudinal intersection: (*17*) Meseta Rio–San Juan Ridge [50], (*18*) Tizayuca Ridge [52], geotraverse 100° W [9]; (f) Central America, Galapagos Islands: (*20*) Nicaragua, Costa Rica, Panama—alkaline basalt [19]; (*21*) Costa Rica, Panama–adakite [19]; (*22*) Galapagos Islands [20, 30]. The GEOROC data base is used. The fields are outlined after [2].

pression of plagioclase as an early crystal phase and the appearance of unusual high-Mg olivine. Using these features, it was concluded that the basaltic andesites and lamprophyres of the Mascota–San Sebastian area were formed from the aqueous melts in oxidized conditions in comparison with the less aqueous and poorly oxidized melts of the volcanic rocks of the Michoacán–Guanajuato region [31]. Because the volcanic rocks of these regions are characterized by different trends (a direct Nb–K correlation in the case of the aqueous and oxidized system and its absence in the relatively dry compositions), it can be suggested that degree of the Nb's mobility (and, probably, the other HFSE elements) increases under the conditions of the water-saturated system.

The rocks of the central block (the Chichinautzin volcanic field, the neighbors of Mexico City, and the Popokatepetl volcano) form two trends: relatively short with direct Nb–K correlation (I) and more variable according to the Nb content (II) without correlation with K (Fig. 7B). The first trend includes the calc-alkaline rocks [56] or the rocks of the first and second volcanic cycles similar in composition [1]. The alkali basalts [56] and the intraplate volcanic rocks of the third type form the second trend. The same difference in the composition and character of the trends is

observed for the high-K basaltic andesites and the andesites enriched in fluid-mobile elements from the frontal zone of the Zitácuaro–Valle de Bravo region and the high-Ti basalts and basaltic andesites of the rear zone of the same region [9]. Based on [9], the association of phenocrysts in the rocks of the first type indicates highly aqueous (3.5–6.5 wt % H_2O) melts, whereas the second type shows relatively dry equilibrium conditions of the minerals–phenocrysts (<1.5 wt %).

Using the same indicative features [9], we may state that the calc-alkaline volcanic type of the Chichinautzin region is aqueous in contrast to the relatively dry intraplate type. The different direction of the trends may be related to the different water saturation and oxidation of the corresponding melts.

The rocks of the eastern block are rather individualized (Fig. 7C). As well as the calc-alkaline (alkaline) rocks of the western blocks, they are characterized by a high K_2O content but are located either in the field of similar compositions of the Hawaiian and Iceland volcanic rocks or occupy an intermediate position relative to the island arc volcanic rocks with direct Nb–K correlation. The so-called riftogenic volcanic rocks of the Meseta Rio–San Juan and Tizayuca fields from the northern and middle parts of the central block are also characterized by correlative trends at high Nb contents but are beyond the Hawaiian–Iceland area (Fig. 7E). Such a particularity of the composition requires a more detail consideration. A similar picture for the alkali basalts of the Central America (Nicaragua, Costa Rica, and Panama) and Galapagos Islands may be seen in Fig. 7F. According to [19], it is observed when the island arc intersects with the mantle plume or is situated rather near its sphere of influence. As was mentioned above, the isotopic data may imply a plume component for the volcanic rocks of the Los Humeros caldera and the El Volcancillo, Los Tuxtlas, El Chichón, and Palma Sola regions. Such a conclusion may be drawn on the basis of the geochemical data for the eastern flank of the TMVB.

The tholeiitic basaltic andesites and Nb-enriched basalts of Baja California with direct Nb–K correlation occupy a similar position within the Hawaiian–Iceland fields (Fig. 7D). The data points of the compositions of the rocks of the San Pedro–Ceboruco graben (the NW block of the TMVB) form subvertical trend (II). The Na-alkali basalts with a plume reservoir marker are located in the field of the Hawaiian–Iceland volcanic rocks (an effect of the Hawaiian plume?), whereas the calc-alkaline rocks of the same trend transit to the island arc area, as in the case of the Michoacán–Guanajuato lava field (Fig. 7A). It is suggested in [47] that the calc-alkaline rocks of the NW block of the TMVB (at least, their lesser differentiated varieties) contain plagioclase as a dominant crystal phase and are free of amphibole in contrast with the majority of the rocks of the same composition from the western block. This evidence of their relatively dry condition may be used for the explanation of the corresponding trend.

Direct correlation between the fluid- (K) and melt-mobile (Nb) components may probably be manifested at the disappearance of the phase boundary in the fluid–melt system. Previously, it was registered for the field of the island arc volcanic rocks resulting from the presence of the fluid- and water-saturated system (trend I). Such a dependence is now observed for the OIB-like compositions. In [19], the melting conditions of the parental melts for the reviewed Central American alkaline rocks are estimated as 1380–1450 °C and 2.7–3.0 GPa (with constraint of the garnet equilibrium). According to the experimental data, the Nb mobility in the fluid–magmatic system significantly increases at high pressures and increased fO_2 values [16]. The transition to the subcritical liquid subject to the equilibrium with garnet considerably increases the mobility of such elements as Nb in the magmatic system [29]. Such an event is probably observed in the plots with trend III.

The so-called bajaites–adakites occupying an isolated position in the field of alkaline island arc volcanic rocks are typical peculiarities of the volcanism of Baja California, the Galapagos archipelago, and Central America. A consideration of the adakite problem, as a commonly accepted indicator of subduction (a result of melting of the oceanic lithosphere), is beyond the limits of our study, because this type of volcanism is widespread locally only in the western and eastern flanks of the TMVB. However, the position of the data points of these rocks in the OIB field rather than in the MORB field and their close relation to the plume reservoir (based on the isotopic data) are astonishing.

The geochemical features of the MORB source, traces of which are absent in the composition of the Mexican basaltic rocks, are typical of the Californian and Galapagos plumes.

SUMMARY AND CONCLUSIONS

1. The subduction origin of the TMVB, envisaging the subduction of the Cocos and Rivera oceanic plates under the North American plate [22, 31], is determined by the classical plate tectonic location of this belt and also mostly by the calc-alkaline volcanism with common island arc features. However, many peculiarities of the tectonics and magmatism of this belt are beyond such a simple model [18, 35, 36, 38, 48]. For example, according to [48], the data points of the isotopic compositions of the Sierra Chichinautzin rocks in the $^{143}Nd/^{144}Nd$–$^{87}Sr/^{86}Sr$ plot are so far from the calculated curve of the mixing of the altered MORB and sediments (well no. 487, Cocos plate) that this excludes their formation due to the partial melting of the subducting plate. Traces of the subduction component are absent both in the isotopic (Fig. 6) and

geochemical (Fig. 7) composition of the TMVB rocks. Even the works with thorough analysis of the subduction influence emphasize the insignificant (no more than 1%) contribution of the subduction component [13].

2. The occurrence of intraplate (OIB) rocks in close spatial and temporal combination with more common calc-alkaline volcanic rocks is a typical peculiarity of the TMVB [33, 35, 36, 56]. However, these authors have different ideas concerning the origin of the OIB-like rocks: (1) a heterogeneous mantle with induced slab convection in the mantle wedge, which causes the advection of the astenospheric mantle [33, 56]; (2) an anomalously heated mantle related to the influx of the material of a rootless mantle plume [36]; (3) an astenospheric OIB-like component [37]; and (4) the origin of the OIB source at the expense of the ascending mantle plume [38].

The calc-alkaline volcanism, locally in association with lamprophyres or alkaline volcanic rocks, is interpreted using different models. The most widespread is a model of the melting of the subduction modified mantle wedge [12, 33, 56]. The origin of the alkaline rocks of the western flank of the TMVB is related to the melting of the mantle source metasomatically enriched in fluid-mobile components, which are traditionally related to the dehydration of the subducted Rivera oceanic plate [12, 33]. It is considered that the lamprophyres are the products of the partial melting of veins of phlogopite pyroxenites in the mantle substrate not differentiated owing to the rapid ascension to the surface during rifting [34]. The models for the Sierra Chichinautzin region are similar to those suggested for the western part of the reviewed territory. One of the models [56] relates the moderately-K composition to the participation of the subduction modified mantle wedge, whereas high-Ti rocks are considered to be formed from the back-arc astenospheric mantle. According to another model [35], the separated leading part of the mantle plume under central Mexico generates high-Ti basaltic melts, and their mixing with the dacitic crustal component is necessary for the formation of moderately-K compositions in this region. Based on [48], the mafic magmas of the Chichinautzin region are the result of the partial melting of the heterogeneous upper mantle, while the andesitic and dacitic magmas are related to the melting of the granulitic source in the lower crust.

The plots shown in Fig. 6 point to two different plume sources of the same type, which belong to intraplate volcanism. For the western part of the TMVB, this is the influence of the Californian plume (Fig. 1), whose traces are recorded in the Na-alkali basalts of the San Pedro–Ceboruco graben; the intraplate basalts of the Michoacán–Guanajuato lava field; and, presumably, the basalts of the Cantaro–Colima area. By their high Nb contents, the compositions enriched in radiogenic Pb (the plume marker) of the first two associations correspond to the products of the Californian plume combined with the area of the most alkaline Hawaiian and Icelandic volcanic rocks (Figs. 7A and 7D). The rest of the data points of the rocks of these associations form a subvertical trend toward the enriched component of the EM-2 (the suggested composition of the sublithospheric mantle) in Fig. 6 and the same trend toward the island arc volcanic rocks in Fig. 7. In the case of the high-Nb rocks of the Cantaro–Colima volcano area, such a trend is weak because of the insufficient data. The isotopic source is not expressed in the composition of the intraplate basalts of the Sierra Chichinautzin area and the Popokatepetl volcano, but such subvertical trends (II) are recorded by the Nb–K proportion.

The eastern part of the TMVB implies the influence of the Galapagos plume. Its isotopic–geochemical traces are recorded in the composition of the alkaline rocks of almost all the volcanic areas at the eastern flank of the TMVB (Figs. 6C and 7C).

The island arc association of calc-alkaline and alkaline rocks is variegated in composition and its each representative may be characterized by different formation conditions. Nonetheless, common peculiarities may be noted for the representative rocks of this association. The conclusion that the andesitic and dacitic magmas (the parental rocks of the island arc association) in the central block of the TMVB (based on the example of the Chichinautzin region) are crustal in origin [48] met a series of criticisms [37]. The basaltic andesites have high MgO and higher Ni contents (Table) and host olivine phenocrysts with inclusions of mantle Cr–Al spinel. The mineralogical and geochemical peculiarities of such basaltic andesites may be related to the partial melting of the depleted lithospheric mantle, which was altered by the fluids [37]. To this must be added the findings of amphibole-bearing lherzolites in the El Penon amphibole andesites (the central block of the TMVB) [8] and the similarity of the compositions of the andesites of the Valle de Bravo–Zitácuaro lava field with the experimental aqueous melts from lherzolites [22]. In Figs. 6 and 7, the isotopic and geochemical plume markers are the part of the trend that transits into the area of the island arc compositions. Consequently, the close spatial–temporal relation may be suggested for the two major magma types—the intraplate and island arc. Probably, the ascending plumes provoke the melting of the subcontinental lithospheric mantle, and the formation of the island arc rocks is mostly related to these magmas. Later, these initial magmas may evolve in the crust according to their own scenario for each area. For example, the slow uplift, volatile evaporation (subvertical trends), and the high degree of crystallinity of the rocks are typical of the intraplate type. Due to their rapid ascent, the island arc magmas retain their primary water (fluid) saturation and high oxidized potential (Nb–K correlation).

3. The rocks of the eastern and especially the western flanks of the TMVB are considerably enriched in fluid-mobile components and are more water-saturated in comparison with the central block (Fig. 7). This is a significant particularity and is beyond the classical model of subduction magmatism and requires its own explanation.

In [37], the authors pay attention to the fact that the results of the widespread alteration of the lithospheric mantle by the mantle plumes may be similar to those related to the subduction. Probably, the influence of both the Californian and Galapagos plumes is manifested in the degree of the mantle's metasomatose on the flanks of the TMVB. It should be outlined, however, that the degree and style of the fluid (water) saturation also depends on the depth of the suggested mantle sources of the western and eastern flanks of the TMVB. This is the level of the spinel–lherzolite equilibrium in the west [18] and the conditions of the equilibrium with garnet in the east [13, 19].

4. The model of the consecutive propagating rifting from the west to the east suggested by some researchers [36, 50] instead of the subduction hypothesis is in agreement with the geological and geophysical data and the isotopic–geochemical peculiarities of the volcanic rocks of the TMVB presented in the given paper. Information on the riftogenic volcanism may be also found for other regions of Northern America [4].

ACKNOWLEDGMENTS

The authors are grateful to A.V. Sobolev for assistance in the obtaining of analytical data.

REFERENCES

1. V. Yu. Kir'yanov, A. V. Koloskov, S. De La Kruz-Reina, et al., "Main Stages in manifestation of the youngest volcanism in the Chichinautzin Zone (Mexican volcanic belt)," Dokl. Akad. Nauk SSSR **311** (2), 432–434 [in Russian].
2. A. V. Koloskov, *Ultrabasic Inclusions and Volcanic Rocks as Self-Regulating Geological System* (Nauch. mir, Moscow, 1999) [in Russian].
3. A. V. Koloskov and G. I. Anosov, "Features of geological structure and Late Cenozoic volcanism of the East Asian margin according to concept of vertical thermodynamics," in *Fundamental Studies of Oceans and Seas*, Ed. by N.P. Laverov (Nauka, Moscow, 2006), Vol. 1, pp. 278–291 [in Russian].
4. S. V. Rasskazov, T. A. Yasnygina, N. N. Fefelov, et al., "Geochemical Evolution of Middle–Late Cenozoic Magmatism in the Northern Part of the Rio Grande Rift, Western United States," Russ. J. Pac. Geol. **29** (1), 15–43 (2010).
5. M. Abratis and G. Worner, "Ridge collision, slab-window formation, and the flux of Pacific asthenosphere into the Caribbean realm," Geol. Soc. Am. **29** (2), 127–130 (2001).
6. A. Aguillon-Robles, T. Calmus, M. Benoit, et al., "Late Miocene adakites and Nb-enriched basalts from Vizcaino Peninsula, Mexico: indicators of East Pacific Rise subduction below Southern Baja California?," Geology **29** (6), 531–534 (2001).
7. M. Benoit, A. Aguillon-Robles, T. Calmus, et al., "Geochemical diversity of Late Miocene volcanism in Southern Baja California, Mexico. Implication of mantle and crystal source during the opening of an asthenospheric window," J. Geol. **110**, 627–648 (2002).
8. D. L. Blatter and I. S. E. Carmichael, "Hornblende peridotite xenoliths from Central Mexico reveal the highly oxidized nature of subarc upper mantle," Geology **26** (11), 1035–1038 (1998).
9. D. L. Blatter, G. L. Farmer, and I. S. E. Carmichael, "A north-south transect across the Central Mexican Volcanic Belt at ~ 1000W: spatial distribution, petrological, geochemical, and isotopic characteristics of Quaternary volcanism," J. Petrol. **48**, 901–950 (2007).
10. K. Bloomfield, "A Late Quaternary monogenetic volcano field in Central Mexico," Geol. Rundsch. **64**, 476–497 (1975).
11. T. Calmus, A. Aguillon-Robles, R. C. Maury, et al., "Spatial and temporal evolution of basalts and magnesian andesites ("bajaites") from Baja California, Mexico: the role of slab melts," Lithos **66**, 77–105 (2003).
12. I. S. E. Carmichael, R. A. Lange, and J. F. Luhr, "Quaternary minettes and associated volcanic rocks of Mascota, Western Mexico: consequence of plate extension above a subduction modified mantle wedge," Contrib. Miner .Petrol **124**, 302–333 (1996).
13. G. Carrasko-Nunez, K. Righter, J. Chesley, et al., "Contemporaneous eruption of calc-alkaline and alkaline lavas in a continental arc (Eastern Mexican Volcanic Belt): chemically heterogeneous but isotopically homogeneous source," Contrib. Mineral. Petrol. **150**, 423–440 (2005).
14. P. R. Castillo, J. W. Hawkins, P. F. Lonsdale, et al., "Petrology of Alarcon Rise lavas, Gulf of California: nascent intracontinental ocean crust," J. Geophys. Res. **107** (B10) (2002).
15. J. Chesley, J. Ruiz, K. Righter, et al., "Source contamination versus assimilation: an example from the Trans-Mexican Volcanic Arc," Earth Planet. Sci. Lett. **195**, 211–221 (2002).
16. C. Dalpe and D. R. Baker, "Experimental investigation of large-ion lithophile-element, high-field-strength-element- and rare-earth-element-partitioning between calcic amphibole and basaltic melt: the effects of pressure and oxygen fugacity," Contrib. Mineral. Petrol. **140**, 233–250 (2000).
17. L. Ferrari, M. Lopez-Martinez, G. Aguirre-Diaz, and G. Carrasco-Nunez, "Space-time patterns of Cenozoic arc volcanism in Central Mexico from the Sierra Madre Occidental to the Mexican Volcanic Belt," Geology **27** ((4)), 304–306 (1999).
18. L. Ferrari, C. M. Petrone, and L. Francalanci, "Generation of Oceanic-Island Basalt-Type Volcanism in the western Trans-Mexican Volcanic Belt by slab rollback, asthenosphere infiltration and variable flux-melting," Geology **6**, 507–510 (2001).

19. E. Gazel, K. Hoernle, M. J. Carr, et al., "Plume-subduction interaction in southern Central America: mantle upwelling and slab melting," Lithos **121**, 117–134 (2011).
20. D. J. Geist, T. R. Naumann, J. J. Standish, et al., "Wolf Volcano, Galapagos Archipelago: melting and magmatic evolution at the margins of a mantle plume," J. Petrol. **46** (11), 2197–2224 (2005).
21. A. Gomez-Tuena, A. LaGatta, C. H. Langmuir, et al., "Temporal control of subduction magmatism in the Eastern Trans-Mexican Volcanic Belt: mantle sources, slab contributions and crustal contamination," Geochem., Geophys., Geosystems **4** (2003). 203GC000524.
22. A. Gomez-Tuena, C. H. Langmuir, S. L. Goldstein, et al., "Geochemical evidence for slab melting in the Trans-Mexican Volcanic Belt," J. Petrol. **48** (3), 537–562 (2007).
23. A. Gomez-Tuena, L. Mori, S. L. Goldstein, et al., "Magmatic diversity of western Mexico as function of metamorphic transformations in the subducted oceanic plate," Geochim. Cosmochim. Acta **75**, 213–241 (2011).
24. K. S. Harpp, V. D. Wanless, R. H. Otto, et al., "The Cocos and Carnegie aseismic ridges: a trace element record of long-term plume-spreading center interaction," J. Petrol. **46** (1), 109–133 (2005).
25. T. Hasenaka and I. S. E. Carmichael, "The cinder cones of Michoacan-Guanajuato, Central Mexico: petrology and chemistry," J. Petrol. **28** ((2)), 241–269 (1987).
26. A. W. Hofmann, "Mantle geochemistry: the message from oceanic volcanism," Nature **385**, 219–229 (1997).
27. K. P. Jochum, D. B. Dingwell, A. Rocholl, et al., "The preparation and preliminary characterization of Eight Geological MPIDING Reverence Glasses for in-situ microanalisys," Geostand. Newslet. **24**, 87–133 (2000).
28. S. T. Johnston and D. J. Thorkelson, "Cocos-Nazca slab window beneath Central America," Earth Planet. Sci. Lett. **146**, 465–474 (1997).
29. R. Kessel, M. W. Schmidt, P. Ulmer, et al., "Trace element signature of subduction-zone fluids, melt and supercritical liquids at 120–180 km depth," Nature **437**, 724–727 (2005).
30. M. D. Kurz and D. Geist, "Dynamics of the Galapagos hotspot from helium isotope geochemistry," Geochim. Cosmochim. Acta **63** (23/24), 4139–4156 (1999).
31. R. A. Lange and I. S. E. Carmichael, "Hydrous basaltic andesites associated with minette and related lavas in Western Mexico," J. Petrol. **31** ((6)), 1225–1259 (1990).
32. J. C. Lassiter and J. F. Luhr, "Osmium abundance and isotope variations in mafic Mexican volcanic rocks: evidence for crustal contamination and constraints on the geochemical behavior of osmium during partial melting and fractional crystallization," Geochem., Geophys., Geosyst. **2** (2001). 2000GC000116.
33. J. F. Luhr, "Extensional tectonics and the diverse primitive volcanic rocks in the Western Mexican volcanic belt," Can. Mineral. **35**, 473–500 (1997).
34. A. H. Maria and J. F. Luhr, "Lamprophyres, basanites, and basalts of the Western Mexican Volcanic Belt: volatile contents and a vein-wallrock melting relationship," J. Petrol. **49** (12), 2123–2156 (2008).
35. A. Marquez, S. P. Verma, F. Anguita, et al., "Tectonics and volcanism of Sierra Chichinautzin: extension at the front of the Central Trans-Mexican Volcanic Belt," J. Volcanol. Geotherm. Res **93**, 125–150 (1999).
36. A. Marquez, R. Oyarzum, M. Doblas, et al., "Alkalic (oceanic island basalt type) and calc-alkalic volcanism in the Mexican Volcanic Belt: a case for plume-related magmatism and propagating rifting at an active margin?," Geology **27**, 1–54 (1999).
37. A. Marquez and C. De Ignacio, "Mineralogical and geochemical constraints for the origin and evolution of magmas in Sierra Chichinautzin, Central Mexican Volcanic Belt," Lithos **62**, 35–62 (2002).
38. G. M. Moore, I. S. E. Carmichael, C. Marone, et al., "Basaltic volcanism and extension near the intersection of the Sierra Madre Volcanic Province and the Mexican Volcanic Belt," Geol. Soc. Am. Bull. **106**, 383–394 (1994).
39. F. Mooser, A. F. M. Nairn, and J. F. W. Negendank, "Paleomagnetic investigations of the Tertiary and Quaternary igneous rocks: VIII. a paleomagnetic and petrologic study of volcanics of Vally of Mexico," Geol. Rundsch. **63**, 451–483 (1974).
40. T. Orozco-Esquivel, C. M. Petrone, L. Ferrari, et al., "Geochemical and isotopic variability in lavas from the Eastern Trans-Mexican Volcanic Belt: slab detachment in a subduction zone with varying dip," Lithos **93**, 149–174 (2007).
41. C. M. Petrone, L. Francalanci, R. W. Carlson, et al., "Unusual coexistence of subduction-related and intraplate-type magmatism: Sr, Nd and Pb isotope and trace element data from the magmatism of San Pedro-Ceboruco Graben (Nayarit, Mexico)," Chem. Geol. **193**, 1–24 (2002).
42. K. Righter and J. Rosas-Elguera, "Alkaline lavas in the volcanic front of the Western Mexican Volcanic Belt: geology and petrology of the Ayutla and Tapalpa volcanic fields," J. Petrol. **42** (12), 2333–2361 (2001).
43. M. C. Rowe, D. W. Peate, and I. U. Peate, "An investigation into the nature of the magmatic plumbing system at Paricutin Volcano, Mexico," J. Petrol. **52** (11), 2187–2220 (2011).
44. P. Schaaf, J. Stimac, C. Siebe, et al., "Geochemical evidence for mantle origin and crustal processes in volcanic rocks from Popocatepetl and surrounding monogenetic volcanoes, Central Mexico," J. Petrol. **46** (6), 1243–1282 (2005).
45. C. R. Stern, F. A. Frey, K. Futa, et al., "Trace-element and Sr, Nd, Pb, and O isotopic composition of Pliocene and Quaternary alkali basalts of the Patagonian plateau lavas of southernmost South America," Contrib. Mineral. Petrol. **104**, 294–308 (1990).
46. B. Stoll, K. P. Jochum, K. Herwig, et al., "An automatediridiumstrip heater for LA-ICP-MS bulk analysis of geological samples," Geostand. Geoanal. Res **32** (1), 5–26 (2008).
47. S. P. Verma and S. A. Nelson, "Isotopic and trace element constraints on the origin and evolution of alkaline

and calc-alkaline magmas in the northwestern Mexican Volcanic Belt," J. Geophys. Res. **94** (B4), 4531–4544 (1989).

48. S. P. Verma, "Geochemistry of evolved magmas and their relationship to subduction-unrelated mafic volcanism at the volcanic front of the Central Mexican Volcanic Belt," J. Volcan. Geotherm. Res **93**, 151–171 (1999).
49. S. P. Verma, "Geochemical evidence for a lithospheric source for magmas from Los Humeros Caldera, Puebla, Mexico," Chem. Geol. **164**, 35–60 (2000).
50. S. P. Verma, "Geochemical evidence for a rift-related origin of bimodal volcanism at Meseta Rio San Juan, North-Central Mexican Volcanic Belt," Geol. Rev **43**, 475–493 (2001).
51. S. P. Verma, "Absence of Cocos plate subduction-related basic volcanism in Southern Mexico: a unique case on Earth?," Geol. Soc. Amer **30** (12), 1095–1098 (2002).
52. S. P. Verma, "Geochemical and isotopic evidence for a rift-related origin of magmas in Tizayuca volcanic field, Central Mexican Volcanic Belt," J. Geol. Soc. India **61**, 257–276 (2003).
53. S. P. Verma and T. Hasenaka, "Sr, Nd, and Pb isotopic and trace element geochemical constraints for a veined-mantle source of magmas in the Michoacan-Guanajuato volcanic field, West Central Mexican Volcanic Belt," Geochem. J. **38**, 43–65 (2004).
54. S. P. Verma and J. F. Luhr, "Sr, Nd, and Pb isotopic evidence for the origin and evolution of the Cantaro-Colima volcanic chain, Western Mexican Volcanic Belt," J. Volcan. Geotherm. Res **197**, 33–51 (2010).
55. N. Vigouroux, P. J. Wallace, and A. J. R. Kent, "Volatiles in high-K magmas from the Western Trans-Mexican Volcanic Belt: evidence for fluid fluxing and extreme enrich melt of the mantle wedge by subduction processes," J. Petrol. **49** (9), 1589–1618 (2008).
56. P. J. Wallace and I. S. E. Carmichael, "Quaternary volcanism near the Valley of Mexico: implications for subduction zone magmatism and the effects of crustal thickness variations on primitive magma compositions," Contrib. Mineral. Petrol. **135**, 291–314 (1999).
57. W. P. Leeman, "Isotopic evolution of lavas from Haleakala Crater, Hawaii," Earth Planet. Sci. Lett. **84**, 211–225 (1987).
58. H. Zou, A. Zindler, X. Xu, and Qu. Qi, "Major, trace element, and Nd, Sr, and Pb isotope studies of Cenozoic basalts in SE China: mantle sources, regional variations, and tectonic significance," Chem. Geol. **171**, 33–47 (2000).

Recommended for publishing by Yu.A. Martynov
Translated by I. Melekestseva